

STRUCTURE AND DYNAMICS OF RARE-GAS LAYERS ON Pt(111)

KLAUS KERN, PETER ZEPPENFELD, RUDOLF DAVID, and GEORGE COMSA

Institut für Grenzflächenforschung und Vakuumphysik,
KFA-Jülich, Postfach 1913, 5170 Jülich (F.R. Germany)

SUMMARY

The structural behavior of rare-gas monolayers on the (111)-surfaces of Ag and of Pt is radically different. On Ag the adlayers show a uniform behavior, they are all "floating" incommensurate. This corresponds to a laterally perfectly flat holding potential; the substrate structure is evidenced only in the alignment of the hexagonal adlayers with the substrate. In contrast, on Pt the adlayers exhibit a great variety of phases and phase transitions. In particular for Xe-adlayers, the phases range from "locked" commensurate and high-order commensurate to various "floating" incommensurate ones. Temperature and coverage changes induce first and second order as well as symmetry breaking and conserving transitions between these phases. This fascinating plurality of phases and phase transitions is due to a delicate balance between the adatom-adatom interaction and the corrugation of the Pt holding potential. This corrugation is thus, in the case of Pt, by no means negligible; its average value - as deduced from direct measurements - is larger than 30 meV, i.e. 10 % of the holding potential.

The lattice dynamics of these rare-gas layers on Pt(111) accessible via the perpendicular modes as observed so far in He inelastic scattering appears to be much less sensitive to the corrugation of the holding potential. All the features predicted by assuming a completely uncorrugated holding potential, i.e. almost dispersionless monolayer mode, leakage into the bulk around $\bar{\Gamma}$ and hybridization with the substrate Rayleigh wave have been confirmed in detail by high resolution He spectroscopy of Ar, Kr and Xe adlayers on Pt(111). No frequency difference between the Einstein oscillations of the commensurate and incommensurate Xe-layers could be detected so far showing that, in spite of the corrugation, the perpendicular curvature of the holding potential does not vary significantly along the surface. Substantial differences are expected for the in-plane adlayer modes.

INTRODUCTION AND STATE OF THE ART

The simplest two dimensional (2D) system which can be imagined is a rare gas monolayer. Such a system cannot be, obviously, realized experimentally; it needs a support. The simplest support is a substrate, which has only to sustain the layer by providing an attractive, laterally perfectly flat potential: a structureless jellium. This is more realistic but still not experimentally realizable to allow for a comparison between theory and experiment. It has been inferred from thermal He scattering experiments that the potential felt by He on close packed metal surfaces (in particular (111)-faces of fcc crystals) is almost ideally flat (corrugation amplitude $\sim 0.01 \text{ \AA}$). These surfaces

have been thus expected to be the closest practical realization of a jellium like substrate for all rare-gases. The extended measurements of the structural and thermodynamical properties of Ar, Kr and Xe layers on Ag(111) as well as their theoretical interpretation (refs. 1,2) appeared to confirm this expectation. The structure of the Ag-substrate seems to have almost no influence on the structure of the various adlayers. In the whole range of temperatures and coverages investigated, the adlayers are incommensurate; their lattice parameter is influenced by temperature and, near monolayer completion (constrained vs unconstrained condition), also by coverage. It is only the azimuthal orientation of the layers, which seemed to disclose that the Ag(111)-substrate is not a structureless jellium but has azimuthal orientation: the adlayers are aligned with the substrate within a few degrees.

The jellium like behavior of Ag(111) as a substrate for rare-gases is, however, not a rule for all close packed metal surfaces. Indeed, rare-gas layers on Pt(111) behave completely differently. In particular Xe adlayers exhibit as a function of temperature and coverage a wealth of structural phases ranging from a commensurate $(\sqrt{3}\times\sqrt{3})R30^\circ$ -hexagonal phase, over striped and hexagonal $R30^\circ$ incommensurate ones, and reaching finally at monolayer completion a hexagonal incommensurate $R30^\circ\pm 3.3^\circ$ -rotated phase (refs. 3,4). The existence of this succession of phases (predicted in ref. 5) has been observed so far only for Xe/Pt(111). The great variety of phases is essentially due to the delicate balance between the mutual interaction of the adatoms and the lateral corrugation of the holding substrate potential felt by the same adatoms.

The (111)-surfaces of Ag and Pt provide apparently two substantially different holding potentials, leading to a correspondingly different structural behavior of the rare-gas adlayers. The adlayers behave in both cases model-like; their structures reflect a perfectly flat and a corrugated support, respectively. The only hint for the origin of this difference can be found so far in the approximately 30% deeper holding potential on Pt than on Ag, from which - according to an empirical rule (ref. 6) - a correspondingly larger lateral potential corrugation may be inferred. A sounder argument has not been provided yet.

Surprisingly, the picture of the dynamical behavior of rare-gas adlayers, supplied so far by inelastic scattering measurements, shows no qualitative difference for Ag(111) and Pt(111) substrates (ref. 7-10). In both cases the experimental results follow in almost every detail the theoretical predictions based on a laterally flat holding potential (ref. 10). The textbook-like correspondence between experiment and theory extends even to the very impressive evolution of the dynamical behavior from mono- to 25-layers films, i.e. from 2D- to 3D-systems. In spite of this, there is so far no detailed explanation

for the fact that the lateral corrugation of the holding potential which influences dramatically the structural behavior is of no consequence for the observed dynamical behavior: rare-gas films on Ag and Pt behave similarly, and there is no measurable difference between the dynamics of the commensurate and the various incommensurate layers on Pt(111) as detected by inelastic He-scattering. This has to be correlated to the fact that the perpendicular adatom motion seems to dominate the cross-section for inelastic He scattering and thus that only perpendicular modes have been measured so far. Differences in the vibrational excitations of commensurate and incommensurate monolayers are certainly expected for in-plane modes. The broken translational invariance of commensurate monolayers ("locked") requires that the longitudinal and transverse phonon branches are optical modes, in contrast to the acoustic nature of these phonon modes in incommensurate monolayers ("floating").

Low energy electron diffraction (LEED) has been used successfully for the study of the structure and thermodynamics of the incommensurate rare gas layers on Ag(111) (refs. 1,2). Particular caution (to avoid electron stimulated desorption of adatoms) and a remarkable skill has been necessary to obtain the bulk of accurate information on adlayer lattice parameter, coverage, multilayer growth, binding energy, etc. It is fair to say that Webb's group has fully exhausted the capabilities of electron scattering for the investigation of rare-gas layers on metals. The energies involved in the excitation of adlayer phonons (3-5 meV) are too small to be well resolved even with the nowadays best electron spectrometers (ref. 12). In addition the possibilities of LEED to study more complicated structures (like striped phases or higher order commensurate layers) are rather limited by the multiple scattering involving substrate atoms: the diffraction pattern becomes exceedingly complex. Complex patterns can certainly be eventually deconvoluted if they are measured with the appropriate statistics; the latter is, however, precluded for many rare-gas/metal systems by the large cross-section for electron stimulated desorption.

High resolution scattering of thermal He-atoms seems to be predestinated for the study of rare gas layers on metal surfaces. This is not only because structural and dynamical information are both accessible in great detail, but in addition, due to the extreme sensitivity of the He scattering with respect to defect and impurities, it allows for a very accurate characterization of the substrate and of the adlayer morphology during the multilayer growth; last but not least thermal energy He has no influence whatsoever even on very unstable adlayer phases.

We will review first the main experimental features of the application of He-scattering for the investigation of rare-gas layers supported on close

packed metal surfaces. Then we will illustrate with a few examples the structural richness of the rare-gas layers on Pt(111). Finally, we will present the picture of the dynamics of rare-gas layers on both Ag(111) and Pt(111) which has been gained so far.

EXPERIMENTAL

The basic capabilities of He-scattering for the investigation of surface structure were already apparent in the early pioneering work of Stern's group in Hamburg in the thirties (ref. 13). However, it was not before the advent of the nozzle-beams that He-beams have become a highly efficient surface investigation tool. The nozzle-beam sources lead simultaneously to a dramatic increase of both the intensity and the monochromaticity of the beams, an achievement comparable only to that of the lasers for light beams. The three main approaches in He-surface scattering allow for an almost exhaustive characterization of rare gas layers: 1) diffraction - for structure (ref. 14), 2) inelastic scattering - for dynamics (ref. 15), 3) and diffuse elastic scattering in combination with interference - for thermodynamics, island formation, defect site occupation, degree of adlayer and substrate perfection (ref. 16).

A modern He surface-scattering spectrometer (see e.g. ref. 17) provides a highly monochromatic ($\Delta\lambda/\lambda \approx 0.7\%$), intensive ($> 10^{19}$ He/sterrad. sec) and collimated ($\Delta\Omega \approx 10^{-6}$ sterrad) He-beam, with energies in the range 10-100 meV. The corresponding wavelength range (1.5-0.4 Å) is well suited for structure determinations which - due to the extreme sensitivity for the outermost layer - can be extended even to shallow, large period adlayer bucklings and matter waves (ref. 18). The resolution attained so far is of the order of 0.01 \AA^{-1} . This is certainly inferior to X-ray performances, but - due again to the superficial sensitivity - the signal/background ratio for the adlayer diffraction peaks is incomparably larger.

The narrow energy spread of the beam in conjunction with a high quality time-of-flight (TOF) system leads to an overall energy resolution for inelastic measurements of less than 0.4 meV at 18 meV beam energy. This and the relatively high cross-section for inelastic events in the range below 15-20 meV makes He-scattering an ideal instrument for the investigation of even detailed features of rare-gas layer phonons (at least of those perpendicularly polarized).

THE STRUCTURE OF RARE-GAS MONOLAYERS

The aim of this section is confined to illustrating the role of the holding potential corrugation in producing the richness of rare-gas layer structures

on Pt(111) mentioned in the introduction. No systematic description of the various structures is intended. The conclusion will be that the nature and richness of these structures imply a relatively strong corrugation of the holding potential and thus, that the rare-gas atoms constituting the commensurate and the incommensurate structure, respectively are in a substantially different energetic environment. This will be contrasted with their apparently rather "uniform" dynamical behavior shown in the next section.

The initially greatest surprise with Xe on Pt(111) was that, in contrast to Ag(111) on which the Xe layer was always floating incommensurate, a $(\sqrt{3}\times\sqrt{3})R30^\circ$ commensurate Xe-layer appeared to be perfectly well locked on the Pt substrate in the whole range $62\text{ K} < T_s < 99\text{ K}$ and $\theta_{\text{Xe}} < 1/3$ ($\theta=1$, represents $1.5\cdot 10^{15}$ adatoms $\cdot\text{cm}^{-2}$, the density of Pt atoms on the (111) surface) (ref. 3). A likewise, $\sqrt{3}$ commensurate Xe structure has been observed on Cu(111) many years ago by Chesters et al. (ref. 19). The basic difference between the two substrates lies in the fact that while the Cu(111) " $\sqrt{3}$ " lattice distance of $d_{\text{Cu}}^{\sqrt{3}} = 4.42\text{ \AA}$ is practically equal to the 4.38 \AA nearest neighbor Xe-bulk distance at $T = 77\text{ K}$, the Pt(111) " $\sqrt{3}$ " lattice distance is $d_{\text{Pt}}^{\sqrt{3}} = 4.80\text{ \AA}$, i.e. almost 10 % too large. This means, that while feeling itself fully "comfortable" (unstrained) on Cu(111) the commensurate Xe layer is highly strained when locked on Pt(111). The remarkable stability of this layer can be explained only by a substantial corrugation of the holding potential. This has been confirmed recently in a molecular dynamics study by Black and Bopp (ref. 20) who have shown that for a holding potential, in which the saddle points are less than 3 meV above the deepest lying (three-fold hollow) sites, the Xe-layer does not become stabilized in the $\sqrt{3}$ -commensurate structure.

The pronounced corrugation of the holding potential on the Pt(111)-surface is obviously not confined to Xe-adatoms. Indeed, we have recently found that the Kr layer undergoes a first order transition from a floating incommensurate to a locked high-order commensurate (5x5) structure at coverages above $\theta_{\text{Kr}} \approx 0.4$ (ref. 18). Although in this structure only 1/6 of the Kr-atoms are located in the energetically most favorable three-fold hollow sites, they are sufficiently strongly held to ensure the locking of the Kr-layer over a temperature range larger than 20 K in spite of the strain produced by the differential thermal expansion.

The $\sqrt{3}$ commensurate Xe-layer on Pt(111) can be destabilized either by cooling below $\sim 62\text{K}$ or by increasing the coverage above $\theta_{\text{Xe}} \approx 1/3$; the layer undergoes transitions into the succession of incommensurate phases mentioned in the introduction. As an example, the second order phase transition from the $\sqrt{3}$ -commensurate phase to the striped structure is shown in fig.1. The illus-

trated phase transition has been obtained by decreasing the surface temperature at constant Xe-coverage, $\theta_{\text{Xe}} \approx 0.30$. The two sequences of polar (left) and azimuthal (right) plots show the evolution of the $(2,2)_{\text{Xe}}$ -diffraction feature; the behavior is reversible. All polar scans shown are taken in the $\overline{\Gamma\text{M}}$ -direction of the Xe-layer; the azimuthal ones are taken at the polar angle corresponding to the maximum of the feature located nearest to the commensurate position (dashed-dotted line). Far above the transition, at 73 K, there is only one sharp peak corresponding to $\sqrt{3}$ -commensurate domains of $\sim 800 \text{ \AA}$. The beginning of the transition is obvious already at 61.5 K. The main peak moves slightly in the polar plot and broadens substantially in the azimuthal plot and an additional peak appears at a larger Q-vector. The azimuthal plot at 60.2 K indicates that the broadening is in fact due to the apparent splitting of the main peak. By further temperature decrease the splitting increases so that at 54 K there is almost no intensity left in between on the $\overline{\Gamma\text{M}}$ -axis; simultaneously, the intensity of the new peak increases, while its position shifts towards larger Q-values. A detailed analysis of 3D-diffraction plots of the $(2,2)_{\text{Xe}}$ - and $(1,2)_{\text{Xe}}$ -features shows that in the incipient stage of the transition a striped phase with superheavy domain walls, running in the $\overline{\Gamma\text{K}}$ -direction, is formed (ref. 21).

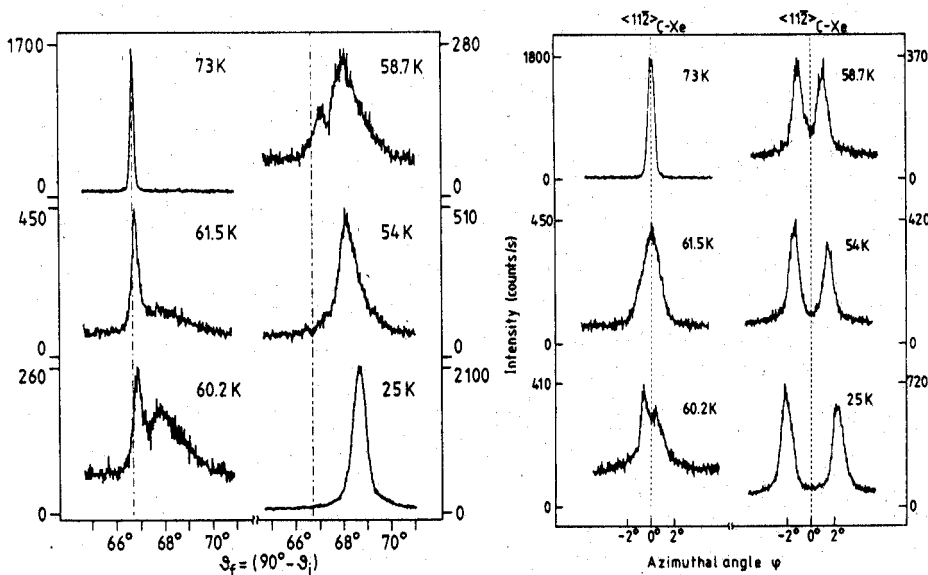


Fig. 1. Polar and azimuthal scans of the $(2,2)_{\text{Xe}}$ diffraction feature at various temperatures during the CI-transition at constant coverage $\theta_{\text{Xe}} \approx 0.30$ ($E_{\text{He}} = 17.4 \text{ meV}$).

In the commensurate phase all Xe-atoms are located at identical sites, more precisely in the energetically most favorable (three-fold hollow) sites of the holding potential. On the other hand, in the incommensurate striped phase the positions of the Xe-atoms are distributed more or less homogeneously over the corrugation of the holding potential; local relaxations might certainly favor to some extent lower lying (more favorable) positions. Thus, the difference of the binding energies of the Xe-atoms in the two phases sets a lower limit for the average corrugation potential. The Xe-coverage dependence of the isosteric heat of adsorption q_{st} of Xe on Pt(111) is shown in fig. 2. The increase of q_{st} with θ_{Xe} , up to commensurate layer completion at $\theta_{Xe} = 1/3$, is due to the mutual attraction between the Xe-adatoms. The ~ 30 meV decrease in heat of adsorption, when θ_{Xe} increases above $1/3$ and the layer becomes incommensurate, represents - as argued above - the lower limit of the average corrugation potential. This is about 10 % of the Xe binding energy and much larger than generally expected. This expectation was based on a not well founded extrapolation. From the almost perfect flatness of close packed metal surfaces for thermal He-scattering it has been inferred that also the holding potential of Xe, Kr or Ar on these surfaces has to be likewise flat. It has been over-seen that, in scattering, He probes the repulsive and not primarily the attractive potential and that the interaction of He with the surface is at least quantitatively very different from that of the heavier rare-gases (e.g. the binding energies for He and Xe on Pt(111) are $\sim 4-6$ meV and ~ 300 meV, respectively). Note that the lower limit of the average corrugation potential deduced from fig. 2 is perfectly compatible with values of activation energy for surface diffusion which represent roughly the potential energy difference between saddle (bridge) sites and three- (or four) fold hollow sites. For instance, the activation energy for surface diffusion of Xe on W(110) (a rather close packed surface) is about 47 meV (ref. 22).

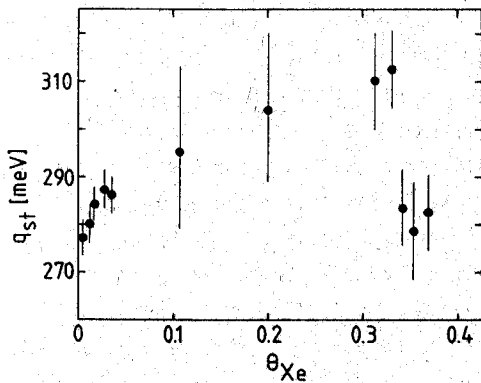


Fig. 2. Isosteric heat of adsorption q_{st} of Xe on Pt(111) as a function of coverage θ_{Xe} .

In summary, we have shown that the holding potential for heavy rare-gases on Pt(111) is substantially corrugated, its average corrugation being at least 10 % of the binding energy. As a consequence the rare-gas adlayers form a rich variety of phases ranging from locked commensurate and high-order commensurate to various "floating" incommensurate ones depending on coverage and temperature. In contrast, on Ag(111) in the whole range of coverage and temperatures only a uniform incommensurate phase aligned with the substrate has been observed so far. The actual reason for this discrepancy is still unclear. The ratio of the rare-gas lattice parameters to that of Ag and of Pt are certainly different; but one may still find, at least for some particular orientation, a situation favorable for adlayer locking. Thus the reason may be found in a much smaller corrugation. If the corrugation scales with the binding energy a reduction of about 30% is to be expected. This would be probably insufficient to explain the dramatic difference in structural behavior.

THE DYNAMICS OF RARE-GAS MONOLAYERS

The first systematic theoretical and experimental exploration of the dynamics of rare gas monolayers on metal surfaces has been performed on Ag(111) (ref. 10). The main conclusion, from the earlier studies of Webb's group (refs. 1,2), allowed for the choice of a very simple adlayer-substrate interaction model: the role of the substrate is just to provide the support for the adlayer by means of a laterally perfectly flat physisorption potential $V(z)$. In a first step the substrate has been considered to be rigid. The interaction between adlayer atoms has been basically modelled by Barker's pair potentials, which are known to do an excellent job in gas phase interactions. They were used in various degrees of sophistication, i.e. from interactions confined to nearest neighbors up to tenth neighbors, with and without relaxation of the static lattice parameters; also the range of the substrate potential $V(z)$ was varied. The calculations supplied dispersion curves fully adequate to account for the available experimental data. The various degrees of sophistication have in fact only a modest impact on the spectra.

As expected from any model involving only central forces between the adatoms and a rigid substrate, the three principal modes of the monolayer decouple, while the perpendicular mode is dispersionless, i.e. the motion of the adatoms perpendicular to the surface acts like an Einstein oscillator. Because the perpendicular surface atom motions dominate the inelastic He cross sections, this dispersionless mode are, indeed, observed in the experiments (refs. 7-10). From the frequency of this mode, one of the three independent parameters of $V(z)$ has been determined, via the second derivative of $V(z)$ at its minimum. (The other two are the depth of the holding potential - obtained

from thermodynamic measurements (refs. 1,2) - and the C_3 coefficient of the z^{-3} van der Waals tail - from calculations by Zaremba and Kohn.) As already mentioned, also for thicker layers (2ML, 3ML and "bulk") the modes observed in experiment - i.e. those involving at least in part perpendicular motions - were adequately accounted for by the calculations. It is particularly impressive to watch how the Rayleigh-wave of the thick, practically semi-infinite solid evolves gradually with increasing layer thickness out of the dispersionless Einstein mode of the monolayer.

It is noteworthy that the most general conclusion, emerging from this study, has been that "coupling between adatom and substrate atom motions is potentially more important than modest variations in the nature of the adatom-adatom potential" (ref. 10). Consistently, Hall, Mills and Black (ref. 11) continued their exploration by allowing now the substrate atoms to move and by focussing on the coupling between the substrate and adlayer modes. In order to avoid the calculation difficulties of the dynamics of an ordered adlayer incommensurate with the ordered substrate, the authors have resorted to the use of two simplifying models. Because the anomalies introduced by the coupling are expected near the $\bar{\Gamma}$ -point, i.e. at wave lengths rather long compared to the substrate lattice parameter, the first model is that of rare-gas layers coupled to the surface of a perfectly smooth, semi-infinite elastic continuum. In the second model, in which the calculations are performed by means of the slab method, the adlayer is assumed to be commensurate with the substrate. Although, the experimental data demonstrate unambiguously that the layer is incommensurate the assumption is defended by the adlayer-substrate lattice parameter being close to $3/2$. A more compelling justification is supplied *a posteriori* by recent measurements on the Xe/Pt(111) system which show that even with the presently attained energy resolution ($\Delta E \sim 0.4$ meV) the energy losses of He-beams scattering from incommensurate and commensurate Xe-layers are indistinguishable. The second model is used to verify the predictions of the first in particular near the zone boundary.

As expected the results of the calculations show that near the zone boundary \bar{M} (the \bar{TM} direction has been explored), where the substrate phonon frequencies are well above those of the adlayer, the influence of the substrate-adlayer coupling is small.

The anomalies introduced by the coupling near the zone center $\bar{\Gamma}$ are two-fold: 1) A dramatic hybridization splitting around the crossing between the dispersionless adlayer mode and the substrate Rayleigh wave (and a less dramatic one near the crossing with the $\omega = c_2 Q_{\parallel}$ line - due to the Van Hove singularity in the projected bulk-phonon density of states); 2) A substantial line-width broadening of the adlayer modes in the whole region near $\bar{\Gamma}$ where

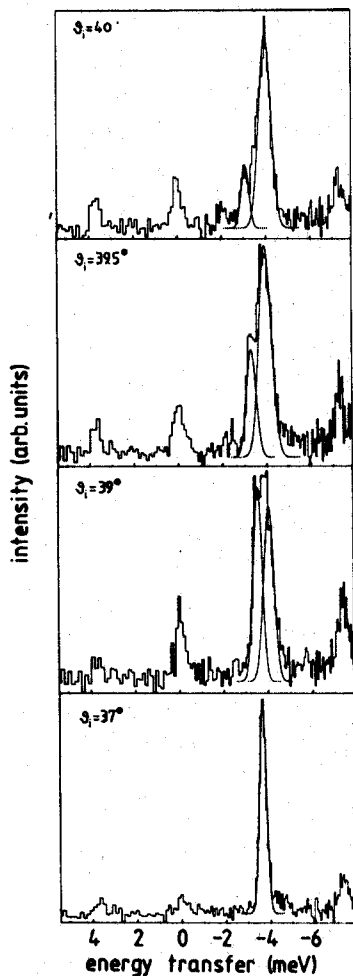


Fig. 3. He energy exchange spectra taken from a Kr monolayer along the $\overline{\Gamma K}_{Kr}$ azimuth at four different incident angles.

they overlap the bulk phonon bands of the substrate: the excited adlayer modes may decay by emitting phonons into the substrate, they become leaky modes. These anomalies were expected to extend up to trilayers even if more pronounced for bi- and in particular for monolayers. More recent experimental data of Gibson and Sibener (ref. 23) confirm qualitatively these predictions at least for monolayers. The phonon line-widths appear to be broadened around $\overline{\Gamma}$ up to half of the Brillouin zone. The hybridization splitting could not be resolved, but an increase of the inelastic transition probability centered around the crossing with the Rayleigh wave and extending up to 3/4 of the zone has been observed and attributed to a resonance between the adatom and substrate modes. In addition, higher-energy transitions were observed to occur at 2 and 3 times the energy of the dispersionless monolayer mode; the authors

noted that they could not decide whether these were due to multiphonon interactions or to overtones.

Recent measurements performed on Ar, Kr and Xe-layers on Pt(111) with a substantially higher energy resolution ($\Delta E \leq 0.4$ meV) have now confirmed the theoretical predictions on the coupling effects within almost every detail (except for the hybridization around the Van Hove singularity, which has not been seen in spite of substantial effort). The sequence of He TOF-spectra in fig. 3 taken along the \bar{TM} direction of the full Kr-monolayer at 25 K gives a vivid picture of the coupling effects (ref. 9). The last spectrum (fig. 3d) taken near the zone boundary \bar{M} exhibits a single, sharp loss at $\Delta E = -3.7$ meV resulting from the creation of a Kr-monolayer phonon (perpendicular Kr-Pt vibration); its width corresponds to the instrumental width of $E_1 = 0.38$ meV, i.e. as expected there is no line-width broadening near zone boundary. On the other hand, the main peak located at $\Delta E = -3.9$ meV in the first spectrum (fig. 3a) taken near the \bar{T} -point and which corresponds also to the creation of a Kr-monolayer phonon is broadened by more than 0.5 meV. Of particular interest is also the small peak at $\Delta E = -3.1$ meV, close to the position of the Pt substrate Rayleigh-wave. The next two spectra (3b and 3c) taken increasingly closer to the crossing between the Pt substrate Rayleigh-wave and the Kr-Einstein mode demonstrate strikingly the effect of the hybridization of the two modes: the originally tiny Pt-peak increases dramatically, while the Kr-peak is pushed slightly toward larger energies. After surpassing the crossover the higher energy loss disappears abruptly. As predicted (ref. 11) the two features in the doublet have comparable intensity only quite near the crossover.

The four plots in fig. 4a show the dispersion of the modes as obtained from TOF-spectra like those in fig.3 taken for mono- ((a) ML), bi- ((b) BL), tri- ((c) TL) and 25-layers ((d) 25 ML) thick films. The hybridization splitting around the crossover with the substrate Rayleigh-wave (solid line) is clearly observed. As predicted, the influence of the coupling to the substrate decreases with increasing layer thickness and is obviously confined to a smaller and smaller fraction of the Brillouin zone, near \bar{T} . The splitting hybridization can be still observed even for the TL. Even the predicted tiny frequency upshift around the \bar{T} -point due to the coupling to the substrate vibrations (ref. 11) is seen in the ML-plot. The sequence in fig. 4a shows again how the Rayleigh-wave of the 25-ML "bulky" film evolves from the originally almost dispersionless ML-mode.

The observed linewidth broadening is shown in fig. 4b. As a measure of the broadening the quantity $\Delta\epsilon = [(\delta E)^2 - E_1^2]^{1/2}$, with δE the full-width-at-half-maximum of the major loss feature, is plotted as a function of the wave-vector. For the ML a broadening larger than 0.5 meV is seen, and - as predicted -

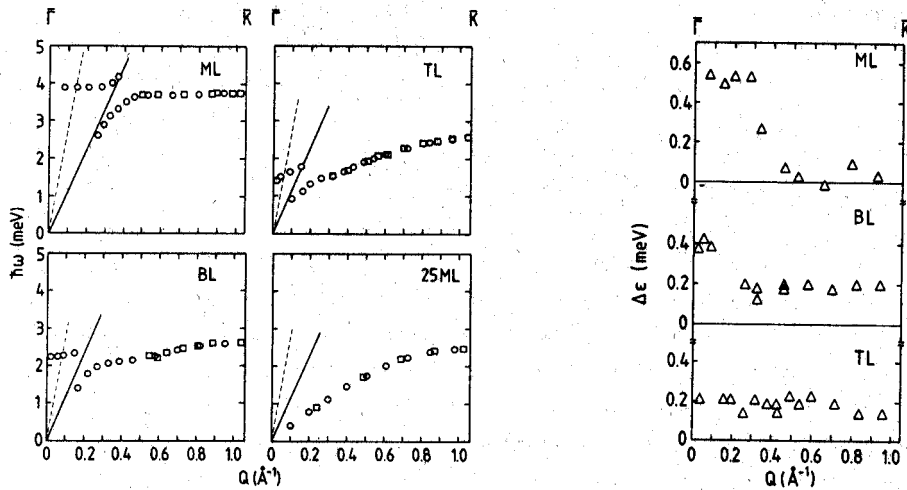


Fig. 4. a) Experimental surface phonon dispersion curves of Kr-films on Pt(111), 1,2,3, and 25 ML thick, measured along the $\overline{\Gamma K_x}$ -azimuth. b) Measured line width broadening $\Delta\epsilon$ of the Kr creation phonon peaks.

confined to the region near $\overline{\Gamma}$, where the adlayer mode overlap the bulk-bands of the substrate. A reduced broadening is still seen in the BL-plot but none in the TL one. Note that while for the ML there is no measurable broadening outside the overlap region - where the adlayer mode ceases to be leaky - for both the BL and TL a broadening of about $\Delta\epsilon \approx 0.2$ meV is present up to the zone boundary. This seems to be due to the fact that the matrix element which controls three-phonon decays (the most probable decay process for a weakly anharmonic lattice) vanishes identically for the ML in a picture which ignores the role of substrate atom motions and the very small three-body forces; for the BL and TL, however, the matrix element is non-zero (ref. 24).

The unresolved question, mentioned above, concerning the origin of the transitions observed to occur at 2 (and 3) times the energy of the ML-mode could be also answered by means of a direct experiment (fig. 5). The figure shows the TOF-spectrum taken from a ML of a perfectly mixed Ar/Kr(1/1) adlayer (ref. 25). In addition to the one phonon creation peaks, Ar(-4.6 meV) and Kr(-3.7 meV) two additional loss peaks are apparent. Their energy corresponds within experimental error to twice the one phonon creation energy for Ar and Kr, respectively. No "mixed" peak (Ar+Kr) is visible, demonstrating that the interactions leading to the double energy loss take place with one single ad-atom only.

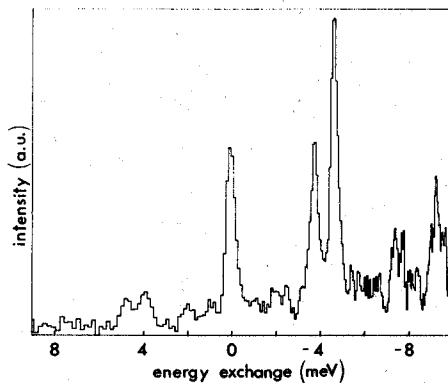


Fig. 5. He energy exchange spectrum taken from a monolayer of a perfectly mixed Ar/Kr(1/1) adlayer.

CONCLUSIONS

The rich variety of the observed structures as well as thermodynamic measurements show that the rare-gas holding potential on Pt(111) is substantially corrugated. On other hand, surface dynamics measurements presented here show in essence that the dynamics of the perpendicular modes of rare-gas adlayers and in particular of monolayers on the close packed Pt(111) surface observed in high-resolution He-inelastic scattering corresponds almost in every detail with theoretical predictions based on the assumption that the holding potential $V(z)$ is perfectly flat. As beautiful this textbook-like correspondence might be, it shows that the dynamics of the perpendicular adlayer modes are not influenced by the lateral corrugation of the holding potential. This is also confirmed by the lack of influence of the commensurate vs incommensurate adlayer structure on the energy losses observed. In spite of the substantial corrugation of the Pt(111) holding potential, its perpendicular curvature appears to be uniform along the surface. Additional information on the actual corrugation of this potential which gives rise to the fascinating variety of adlayer structures, will be thus in principle obtainable from inelastic measurements only if also longitudinal modes become accessible to the experiment.

REFERENCES

- 1 J. Unguris, L.W. Bruch, E.R. Moog and M.B. Webb, *Surf. Sci.* 87 (1979) 415-436
- 2 J. Unguris, L.W. Bruch, E.R. Moog and M.B. Webb, *Surf. Sci.* 109 (1981) 522-556
- 3 K. Kern, R. David, R.L. Palmer, and G. Comsa, *Phys. Rev. Lett.* 56 (1986) 620-623
- 4 K. Kern, *Phys. Rev.* B35 (1987) 8265-8268
- 5 P. Bak, D. Mukamel, J. Villain, and K. Wentowska, *Phys. Rev.* B19 (1979) 1610-1613
- 6 G. Ehrlich, in *Chemistry and Physics of Solid Surfaces Vol. III*, R. Vanselow and W. England (Eds.), CRC Press, Boca Raton, 1982, p. 61

- 7 K.D. Gibson and S.J. Sibener, Phys. Rev. Lett. 55 (1985) 1514-1517
- 8 K. Kern, R. David, R.L. Palmer, and G. Comsa, Phys. Rev. Lett. 56 (1986) 2823-2826
- 9 K. Kern, P. Zeppenfeld, R. David, and G. Comsa, Phys. Rev. B35 (1987) 886-889
- 10 K.D. Gibson, S.J. Sibener, B.M. Hall, D.L. Mills, and J.E. Black, J. Chem. Phys. 83 (1985) 4256-4270
- 11 B.M. Hall, D.L. Mills, and J.E. Black, Phys. Rev. B32 (1985) 4932-4945
- 12 H. Ibach, J. Vac. Sci. Technol. A5 (1987) 419-423
- 13 I. Estermann and O. Stern, Z. Phys. 61 (1930) 95-125
- 14 T. Engel and K.H. Rieder, Springer Tracts in Modern Physics, Vol. 91, Springer, Berlin, 1982
- 15 J.P. Toennies, J. Vac. Sci. Technol. A2 (1984) 1055-1065
- 16 G. Comsa and B. Poelsema, Appl. Phys. A38 (1985) 153-160
- 17 R. David, K. Kern, P. Zeppenfeld, and G. Comsa, Rev. Sci. Instr. 57 (1986) 2771-2779
- 18 K. Kern, P. Zeppenfeld, R. David, and G. Comsa, Phys. Rev. Lett. 59 (1987) 79-82
- 19 M.A. Chesters, M. Hussain, and J. Pritchard, Surf. Sci. 35 (1973) 161-171
- 20 J.E. Black and B. Bopp, Phys. Rev. B34 (1986) 7410-7412
- 21 K. Kern, R. David, P. Zeppenfeld, R.L. Palmer, and G. Comsa, Solid State Comm. 62 (1987) 391-394
- 22 J.R. Chen and R. Gomer, Surf. Sci. 94 (1980) 456-468
- 23 K.D. Gibson and S.J. Sibener, Faraday Discuss. Chem. Soc. 80 (1985) 203-215
- 24 D.L. Mills, private communication
- 25 P. Zeppenfeld, K. Kern, R. David, and G. Comsa, to be published